

Supplementary Material

Using the Fast Fourier Transform in Binding Free Energy Calculations

Trung Hai Nguyen ^{*}, Huan-Xiang Zhou [†], David D. L. Minh [‡]

September 23, 2017

^{*}Department of Chemistry, Illinois Institute of Technology, Chicago, IL 60616, USA

[†]Departments of Chemistry and Physics, University of Illinois at Chicago, Chicago, IL 60607, USA

[‡]Department of Chemistry, Illinois Institute of Technology, Chicago, IL 60616, USA

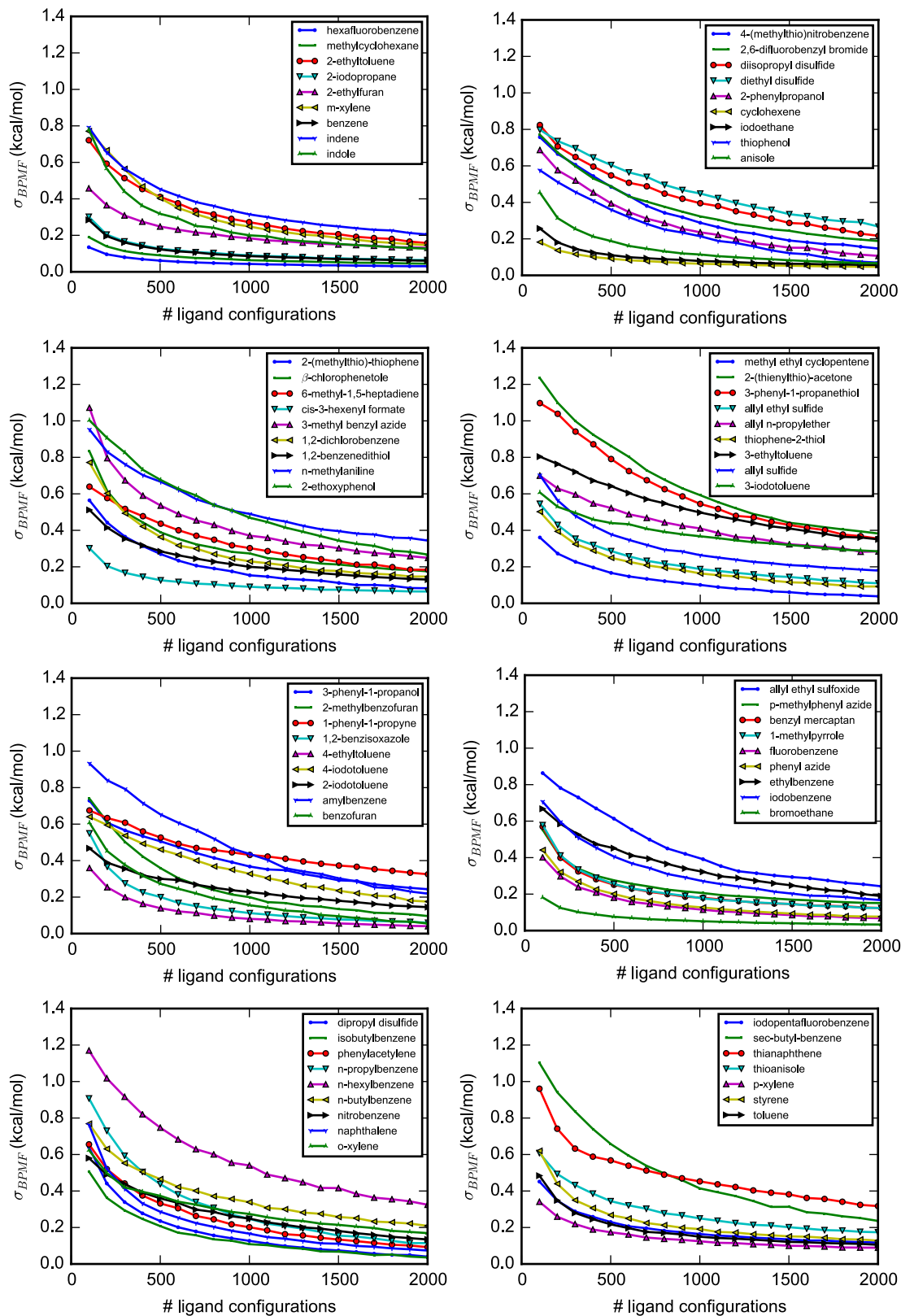


Figure S1: Convergence of BPMF calculations. Standard deviations (σ_{BPMF}) of BPMF calculations as a function of the number of ligand configurations, shown for 70 active ligands. σ_{BPMF} are estimated by bootstrapping, taking the standard deviation of N configurations sampled with replacement from the total pool of ligand configurations.

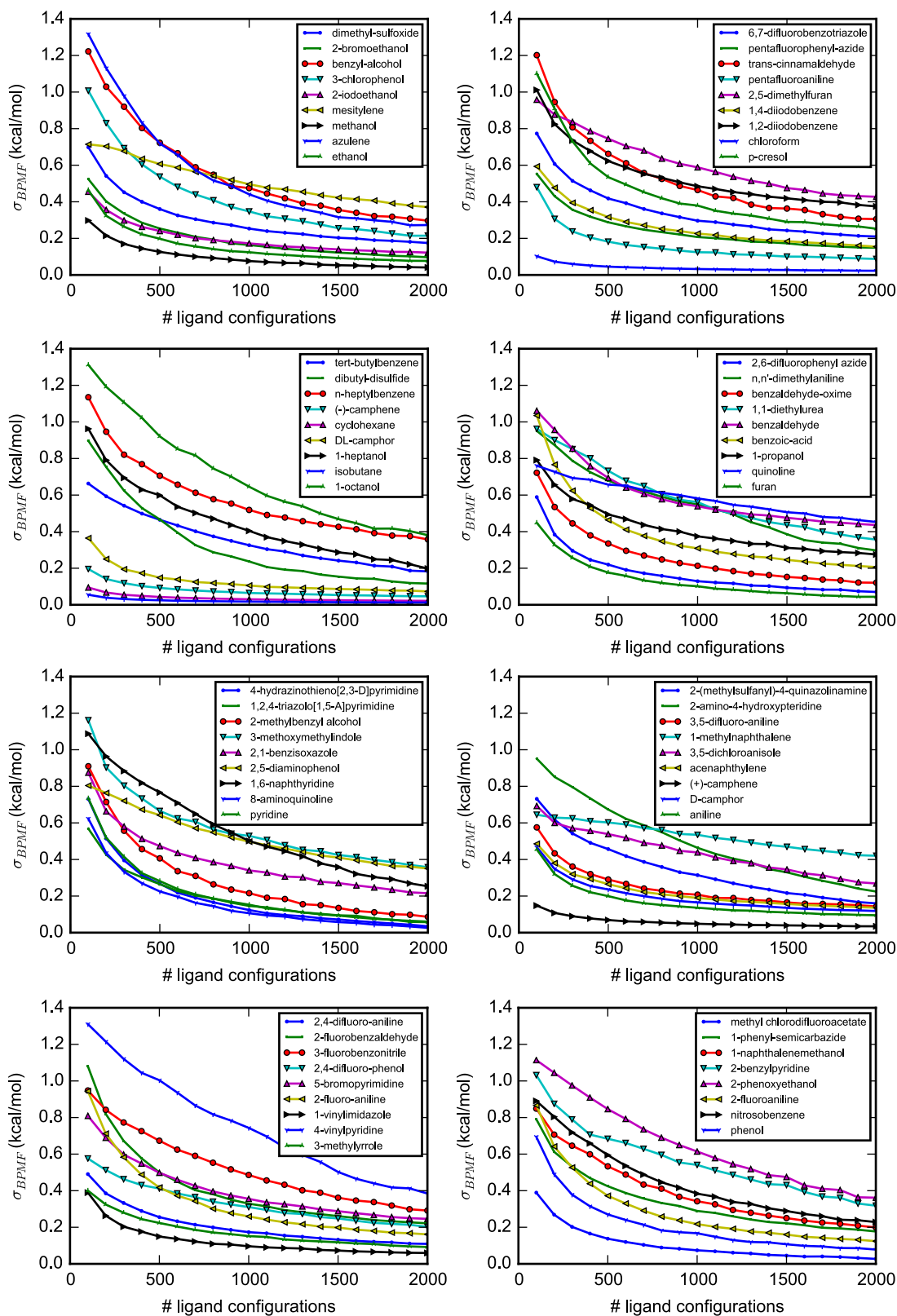


Figure S2: Convergence of BPMF calculations. Standard deviations (σ_{BPMF}) of BPMF calculations as a function of the number of ligand configurations, shown for 71 inactive ligands. σ_{BPMF} are estimated by bootstrapping, taking the standard deviation of N configurations sampled with replacement from the total pool of ligand configurations.

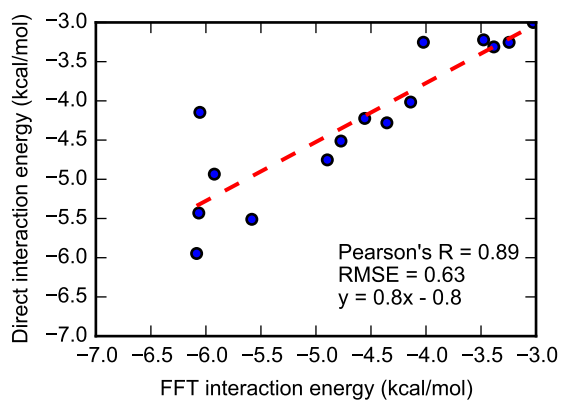


Figure S3: FFT-based vs direct interaction energies between benzene and a snapshot of T4 lysozyme with a grid spacing of 0.8 Å.

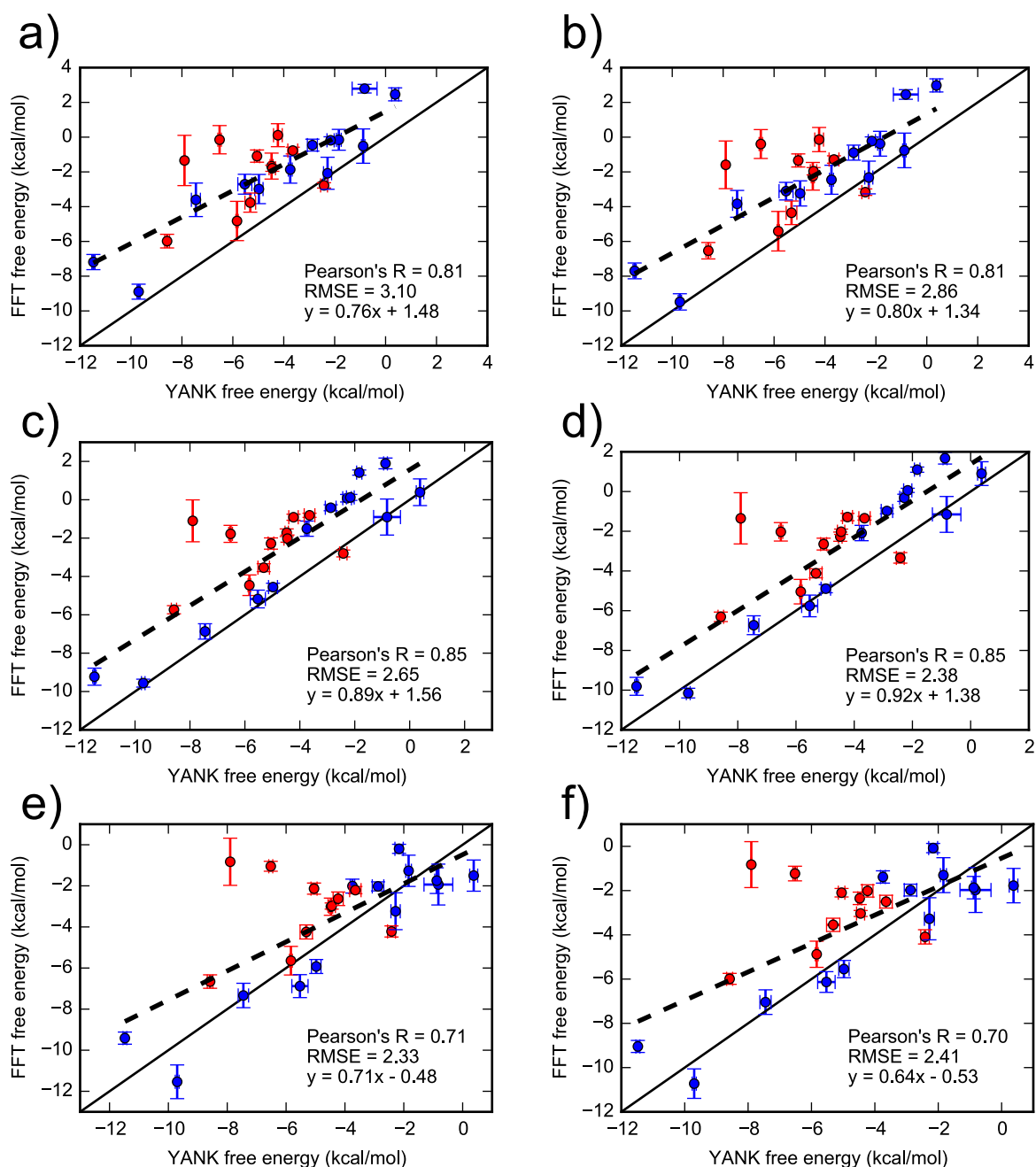


Figure S4: Comparing binding free energies for 24 ligands estimated using YANK (x-axis) and FFT Δ G (y-axis). For the FFT Δ G calculations, the grid spacing was 0.25 Å and grid size was 16 Å cubed, encompassing only the binding pocket. Active and inactive molecules are shown with red and blue markers, respectively. The labels (a) to (f) correspond to different weighting schemes. Error bars denote the standard deviation from three independent YANK calculations (x-axis) or from bootstrapping BPFs (y-axis), with the range of error bars representing a single standard deviation. The solid line is $y = x$ and the dashed line is a linear regression based on all data points.

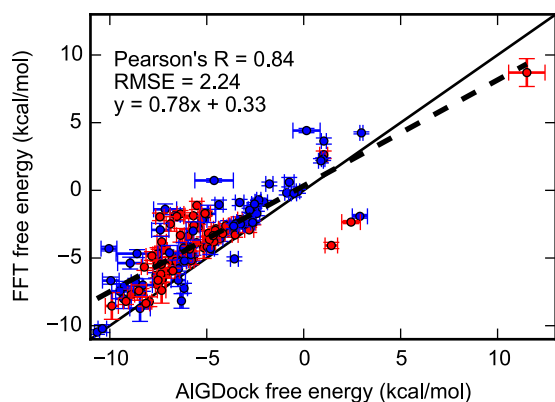


Figure S5: Binding free energies for 141 ligands estimated using AIGDock (x-axis) and FFT (y-axis) using weighting scheme (c). For FFT calculations, the grid spacing was 0.125 \AA and grid size was 16 \AA cubed, encompassing only the binding pocket. Active and inactive molecules are shown with red and blue markers, respectively. Error bars denote the standard deviation from bootstrapping BPMFs, with the range of error bars representing a single standard deviation. The solid line is $y = x$ and the dashed line is the linear regression line.

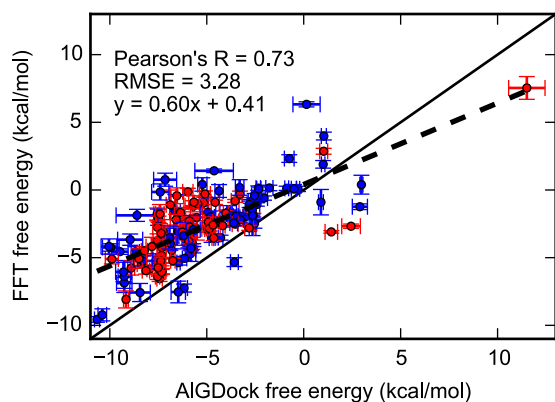


Figure S6: Binding free energies for 141 ligands estimated using AIGDock (x-axis) and FFT ΔG (y-axis) using weighting scheme (c). For FFT calculations, the grid spacing was 0.25 \AA and grid size was 16 \AA cubed, encompassing only the binding pocket. Active and inactive molecules are shown with red and blue markers, respectively. Error bars denote the standard deviation from bootstrapping BPMFs, with the range of error bars representing a single standard deviation. The solid line is $y = x$ and the dashed line is linear regression line.

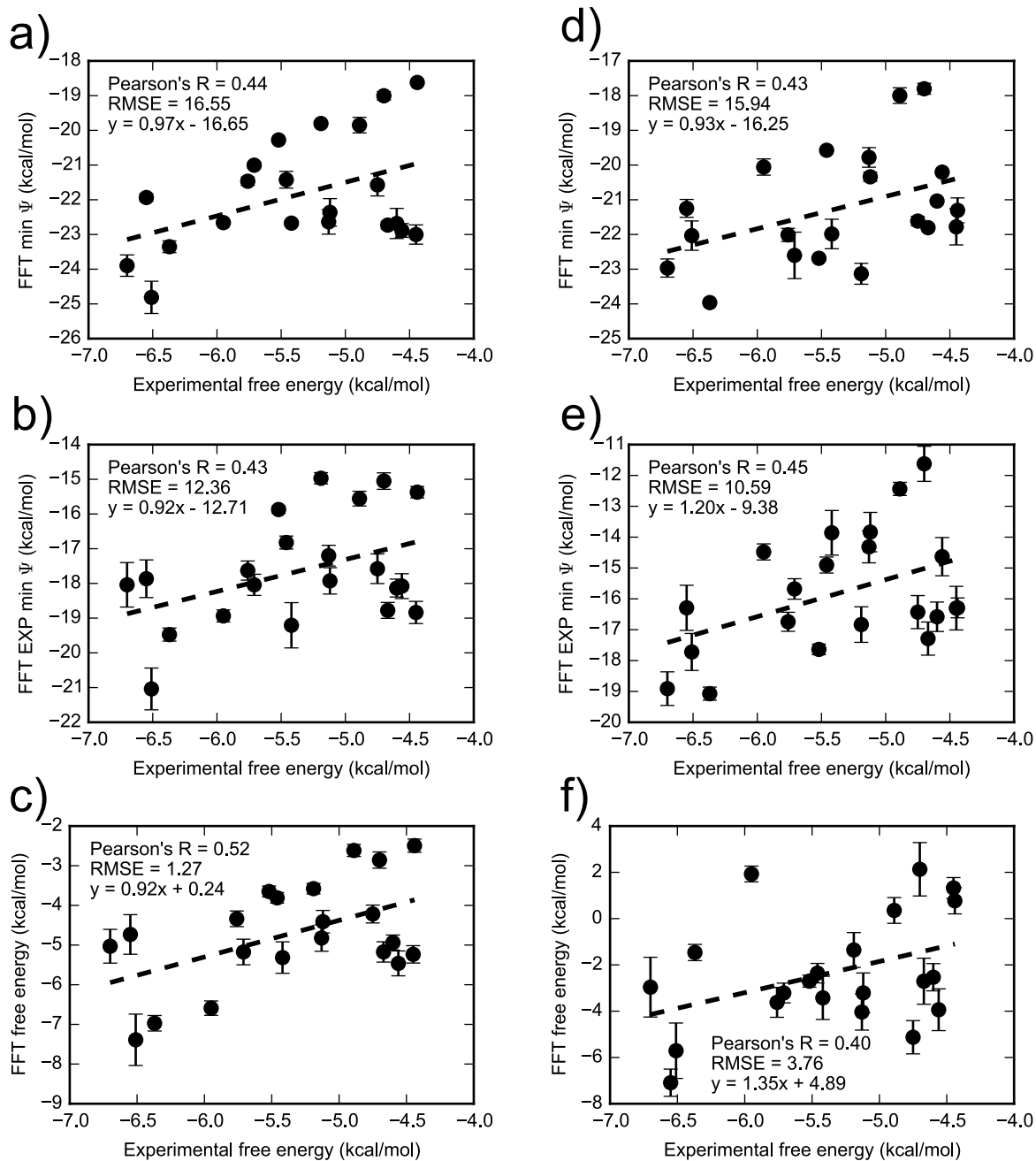


Figure S7: Comparing FFT free energy calculations in (a-c) OBC2 and (d-f) PBSA implicit solvent with experiment for 21 ligands. The top row are minimum interaction energies for all receptor snapshots, middle row are the exponential average of the interaction ψ energies, and bottom row are the full FFT ΔG estimate. Note that each set of axes have different limits. Figure 11 in the main is similar but excludes the outlier iodobenzene.

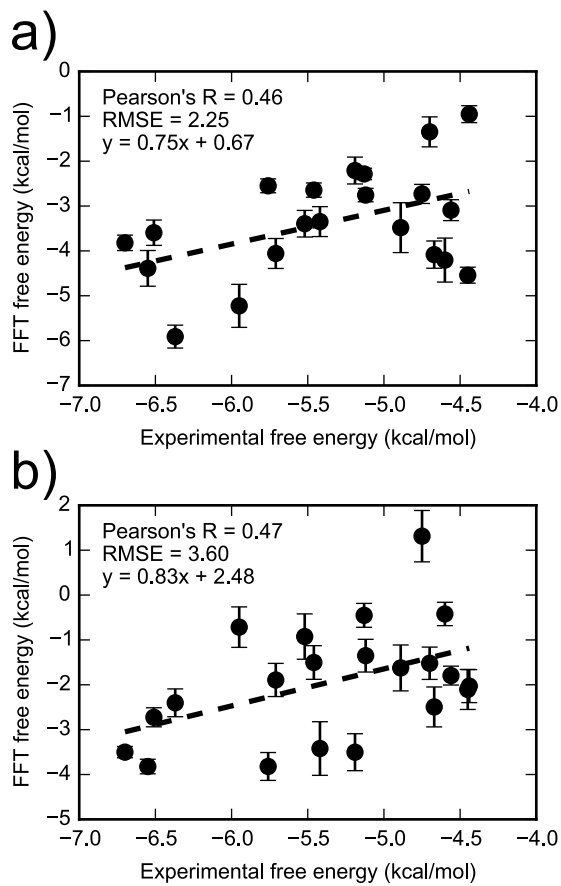


Figure S8: Comparing FFT free energies with experiment. The FFT free energies were estimated with large grid size ($62 \text{ \AA} \times 62 \text{ \AA} \times 62 \text{ \AA}$) in OBC2 (a) and PBSA (b) implicit solvents. In contrast to Fig. 12 in the main text, this figure includes iodobenzene.

References

- [1] Weininger, D. *J. Chem. Inf. Comput. Sci.* **1988**, *28*, 31–36.